Engineering Science and Technology, an International Journal 21 (2018) 611–624

HOSTED BY

Contents lists available at ScienceDirect

Engineering Science and Technology, an International Journal

journal homepage: www.elsevier.com/locate/jestch

Full Length Article

A collaborative representation face classification on separable adaptive directional wavelet transform based completed local binary pattern features

Mohd. Abdul Muqeet [a,b,*], Raghunath S. Holambe [b]

[a] Electrical Engineering Department, Muffakham Jah College of Engineering and Technology, Hyderabad, TS, India
[b] Department of Instrumentation Engineering, SGGS Institute of Engineering and Technology, Nanded, MS, India

ARTICLE INFO

Article history:
Received 17 August 2017
Revised 26 April 2018
Accepted 14 May 2018
Available online 28 May 2018

Keywords:
Face recognition
Separable adaptive directional wavelet transform
Completed local binary patterns
Collaborative representation classification

ABSTRACT

Face recognition has emerged as the most active area of research in computer vision. A variety of face recognition methods were devised, though several challenges are imposed due to face variations such as facial expression, pose variation and illumination variation which generate great concern in developing efficient face recognition methods. It is desirable to extract robust local descriptive features to effectively represent such face variations. The essential attribute of the proposed method is to extract directional descriptive local features based on the face image characteristics. In order to extract the multi-resolution directional features as per the face variations, a 2-D interpolation-based separable adaptive directional wavelet transform (SADIWT) is proposed. For the implementation of 2-D SADIWT, a set of seven directions with an improved quadtree partitioning scheme is proposed. Completed local binary patterns (CLBP) superior to local binary patterns (LBP) in extracting local texture features are applied on top level's 2-D SADIWT sub-bands to obtain local descriptive features. Collaborative representation classification (CRC) takes benefit of these descriptive features and leads to a very competitive classification performance. Extensive experimental results on benchmark face databases such as ORL, FERET, CMU-PIE, and LFW demonstrate high classification accuracy of the proposed method. A comparison with numerous methods which include various holistic, LBP-based descriptors and representation methods demonstrate the efficacy of the proposed method. Experiments are also conducted to exhibit the robustness and discrimination capability of the proposed method for handling single image per person (SIPP) and random block occlusion problem.

1. Introduction

During the last three decades, numerous face recognition approaches have been devised which perform well under restricted conditions. Face images captured under uncontrolled practical scenarios are influenced by different facial variations such as expressions, poses, occlusions, and illumination [1]. Therefore extracting robust features is essential for efficient face recognition systems. Face representation and classification are the two most essential points in the development of any face recognition system. Face representation deals with the extraction of unique features from the face images and performs a noteworthy function in the improvement of performance of a face recognition system. A dominant face representation method must be discriminative for different subjects and invariant to different face variations. Prominent holistic-based face representation methods comprise of Eigenfaces using principal component analysis (PCA) [2], Fisherfaces using linear discriminant analysis (LDA) [3,4], and locality preserving projections (LPP) [5]. Generally, the holistic methods are sensitive to the aforesaid facial variations. Among local descriptors, local binary patterns (LBP) are successfully implemented for facial feature extraction [6,7] and offer simple implementation and tolerance against illumination. The limitation of the LBP-based method is its sensitivity towards the noise. To describe the local textures more in detail, Guo et al. [8] proposed completed local binary pattern (CLBP) and established its efficacy in texture feature extraction as compared to LBP. Weber local descriptors (WLD) [9] are other powerful local descriptors. Zhang et al. [10] used the WLD to extract local facial features from predefined facial landmarks and efficiently captured pose-invariant features. Wang et al. [11]

* Corresponding author at: Electrical Engineering Department, Muffakham Jah College of Engineering and Technology, Road No.3, Banjara Hills, Hyderabad 500034 TS, India.
E-mail address: ab.muqeet2013@gmail.com (M.A. Muqeet).
Peer review under responsibility of Karabuk University.

https://doi.org/10.1016/j.jestch.2018.05.008
2215-0986/

developed an effective classification method using Locality-constrained linear coding (LLC). Although LBP, WLD, and LLC show promising results, they still confront with many limits and challenges, such as the small sample size (SSS problem) and face misalignment induced by pose variations [10]. Researchers applied pre-processing methods prior to LBP computations to improve the face recognition performance. Numerous multi-resolution analysis (MRA) methods are combined with LBP to extract MRA-based local descriptive features. Local Gabor binary pattern (LGBPHS) [12] is one such eminent MRA-based local facial descriptor which combines the Gabor filters with LBP. However, LGBPHS generates large dimension feature vector. In [13], LBP coded image of curvelet transformed low-frequency approximation sub-band and normalized mid-frequency sub-bands are considered to form the feature set and later LPP is used for dimensionality reduction. But multi-region local feature details are not extracted to confront different face variations. Alelaiwi et al. [14] proposed a face recognition system based on SPT and LBP for e-Health secured login for patients. SPT sub-bands are generated with different scales and orientations. LBP is applied to each of the sub-band to extract histogram features. Later local learning based algorithm (LLB) is applied to reduce the dimensionality of generated features. Patil et al. [15] proposed a novel feature fusion technique and considered the contourlet transform and performed multi-block LBP and multi-block WLD histogram feature extraction. However, application of two local descriptors increases the complexity of this method. Moreover, these methods [12–15] use MRA methods which despite capturing the directional information lack the adaptation in selecting the directional details based on the face image characteristics and suffer from various issues such as high computational rate and complex filter design.

Adaptive MRA methods of approximation are regarded to be more compact than the non-adaptive ones since the optimal directions as per the image characteristics are selected adaptively through the approximation process [17]. The prominent adaptive MRA methods which adaptively decide filtering directions as per the description of images have been proposed in [16–18]. Chang et al. [16] developed a direction-adaptive discrete wavelet transform (DA-DWT) for image compression where only one pair of lifting step and non-interpolated integer samples are used to realized directional lifting and Neville filters [21] are used as the prediction and update filters. Ding et al. [17] suggested adaptive directional lifting (ADL) based separable wavelet transform which could be implemented with one or two pairs of lifting steps with 5/3 or 9/7 CDF wavelet filters [21]. Maleki et al. [18] proposed directional wavelets (DIW) with megaquad partitioning algorithm in the adaptive directional lifting based framework to efficiently capture edge features. Adaptive filter direction selection as per the image characteristics makes these methods efficient in approximating directional features. Moreover, as a result of lifting based factorization, perfect reconstruction is also assured and the resultant multi-resolution image is absolutely compatible with that of the conventional 2-D DWT multi-resolution image. Recently, Muqeet and Holambe utilize the DA-DWT [16] for facial feature extraction [19] and compared its effectiveness with famous subspace and non-adaptive MRA-based face recognition methods. Very recently in [20], LBP histogram features are extracted from the directional wavelet transform sub-bands. LDA is used as the dimensionality reduction method.

Classification using a robust classifier is a pivotal step to attain a superior performance for any face recognition method. Nearest neighbor (NN) classifier [23] is the most widely used classifier which classifies the testing face image according to the nearest training face image. But NN classifier is unstable as it uses less information of training set to assess the testing image. Recently, some classification methods such as sparse representation classification (SRC) [24], collaborative representation classification (CRC) [25], and linear regression classification (LRC) [26] have been devised which substantially improve the classification performance. Zhang et al. [25] verified that CRC attains a superior classification performance as compared to SRC. While performing classification, CRC not only considers the similarity between training samples but also considers the correlation among the training samples. Due to this CRC can be effectively utilized for face recognition even under uncontrolled environments. The performance of LRC is confined as it does not entirely utilize the discrimination information of the training samples. Both CRC and SRC and its variant have been extensively used in face recognition methods [27–31]. Cao et al. [27] used the sparse representation for extraction of illumination and pose-invariant features. Fan et al. [28] improved the SRC method by computing the weight of training samples and obtained superior results compared to SRC and CRC methods. Liu et al. [29] used hierarchical multi-scale LBP and performed classification using sparse coding with the application of a matching pursuit-based greedy search approach. Wang et al. [30] combined the Gabor wavelet transform (GWT) and CLBP features and carried out the SRC to perform classification.

The motivation of the proposed method is to develop an efficient facial feature extraction method which considers the different facial variations and captures significant directional information from the face images. Accordingly, considering the benefit of directional lifting and adaptation in direction selection based on the image characteristic, this paper proposes to develop a 2-D interpolation-based separable adaptive directional wavelet transform (SADIWT) to extract multi-resolution directional information from the face images. While implementing 2-D SADIWT, seven directions with an improved quadtree partitioning scheme are proposed. The contribution of the proposed work is threefold. At first, different multi-resolution sub-bands are obtained by applying the proposed 2-D SADIWT. Secondly, histograms features using sign-magnitude differences of the CLBP [8] are extracted from the selected top-level's 2-D SADIWT sub-bands. The 2-D SADIWT detects the edges adaptively as per image characteristics and the CLBP captures the distribution of various local micro-patterns from these sub-bands, for instance, edges, spots, and flats. Lastly motivated by the benefits offered by the collaborative representation for efficient face classification, it is utilized to perform robust classification. There are two benefits of the proposed method: firstly, it can fully utilize the CLBP functionality i.e. CLBP-based histogram features extracted from the 2-D SADIWT sub-bands are more descriptive, illumination invariant, and can significantly reduce redundant information and make the method computationally efficient. Secondly, CRC can perform efficiently on these local descriptive features and contribute to improving the overall classification accuracy. The remaining part of the paper is arranged as follows. Implementation of the proposed 2-D SADIWT using proposed seven directions with an improved quadtree partitioning scheme and associated theory of CLBP and CRC is explained in section 2. Further, the proposed facial feature extraction method is discussed in section 3. In section 4, parameter settings are discussed and experimental results are performed on four widely used face databases. Conclusions based on the experimental results are discussed in section 5.

2. Materials and methods

In this section, the implementation of the proposed 2-D SADIWT in the proposed seven directions using the improved quadtree partitionning scheme is illustrated. A related theory on CLBP and CRC is also explained and their individual contribution to the proposed method is also described.

2.1. Implementation of 2-D separable adaptive directional wavelet transform(2-D SADIWT)

The fundamental concept of implementation of our proposed method is to carry out transform operations on a face image at a viable variety of possible directions while maintaining the characteristics of multi-resolution, localization, and isotropy intact. This section describes the extraction of directional details from the face images using the proposed 2-D interpolation-based separable adaptive directional wavelet transform (SADIWT) which considers proposed set of seven directions with an improved quadtree partitioning scheme. The implementation of proposed 2-D SADIWT utilizes the concept of directional lifting for which the readers are directed to [16–19]. The 2-D SADIWT still performs two separable 1-D horizontal or vertical conventional lifting wavelet transform [21] but consist of modification in the prediction and update step. 2-D SADIWT is realized with only one pair of lifting step, which means only one prediction step followed by one update step [16]. Furthermore, the sub-pixel interpolation is performed for non-integer samples within the image sampling grid. Let $x[i,j]$ be a 2-D face image which is first decomposed by the 1-D SADIWT in the vertical direction and then in the horizontal direction. Each 1-D SADIWT is factored into one lifting stage which mainly comprises split, predict and update steps. In the split step, the image $x^e[i,j]$ is first vertically sub-sampled to get even $x^e[i,j] = x[i,2j]$ sub-samples and odd $x^o[i,j] = x[i,2j+1]$ sub-samples. In the prediction step of 1-D SADIWT, odd samples $x^o[i,j]$ are predicted from neighboring even row samples along an optimal direction θ. The prediction of each odd sample is a linear combination of neighboring even samples with a strong correlation in the direction θ. Here samples from six nearest even rows are selected to take part in the prediction step. The prediction operator $P(\cdot)$ and the generated high-pass signal $H[i,j]$ are described in (1) and (2) respectively,

$$P(x^o)[i,j] = \sum_{n=-K_p}^{K_p-1} W_n^p . x^e[i + sign(n-1)tan\theta, j+n] \tag{1}$$

$$H[i,j] = g_H(x^o[i,j] - P(x^o)[i,j]) \tag{2}$$

Where $sign(x) = 1$ for $x \geq 0$ and -1 otherwise. $2K_p$, W^p, and g_H are the length of the prediction filter, coefficients of the prediction filter, and the scaling factor respectively. Now in update step, even samples $x^e[i,j]$ are updated from odd samples of high pass signal along the same optimal direction θ. The update operator $U(\cdot)$ and the generated low-pass signal $L[i,j]$ are described in (3) and (4) respectively,

$$U(H)[i,j] = \sum_{n=-K_u}^{K_u-1} W_n^u \cdot \begin{pmatrix} x^o[i + sign(n)tan\theta, j+n] - \\ P(x^o)[i + sign(n)tan\theta, j+n] \end{pmatrix} \tag{3}$$

$$L[i,j] = g_L(x^e[i,j] + g_H^{-1}(U(H^o)[i,j])) \tag{4}$$

where $2K_u$, W^u, and g_L are the length of the update filter, coefficients of the update filter, and scaling factor respectively. The values of $g_L = 1.342$ and $g_H = 0.707$ are considered as given in [16]. For the implementation of 2-D SADIWT, Neville filters with six vanishing moments [22] are utilized as prediction and update filters i.e. $K_p = K_u = 3$. Referring to [41] for a two channel lifting filter bank with an order of $N = 6$ for both dual and primal vanishing moments, the prediction filter coefficients can be obtained by considering the value of $M = 2$ and shift $\tau = i/M = -1/2$ [22] as given in (5),

$$P_i(z) = \sum_{i=1}^{N/2} W_i(z^{-i} + z^{i-1}),\ W_i = \frac{(-1)^{i+\frac{N}{2}-1}\prod_{k=1}^{N}(\frac{N}{2}+0.5-k)}{(\frac{N}{2}-i)!(\frac{N}{2}-1+i)!(i-0.5)} \tag{5}$$

Using (5) the coefficients of the prediction filter can be obtained as $W^p = [3,-25,150,150,-25,3]/2^8$. Using Theorem 3 [22], the coefficients of update filter can be obtained as $W^u = [3,-25,150,150,-25,3]/2^9$. These filters possess linear phase characteristics which increase their texture discrimination capability and also performing lifting wavelet transform with these high vanishing moments filters increases the approximation power of the 2-D SADIWT. For the proposed method a set of seven directions is proposed to take part in the prediction and update steps as given in (6),

$$\Theta = \{\theta | \theta = 0, \pm 22.5, \pm 45, \pm 67.5\} \tag{6}$$

These directions are considered to confirm a strong correlation among samples and to capture dominant directional features from the face images. It is to note that the term $sign(n-1)tan\theta$ (1) and (3) may not always be an integer sample and does not exist on the original image sampling grid. Consequently, an interpolation method is carried out to estimate the intensity for these non-integer or fractional samples. For perfect reconstruction, the integer samples used to interpolate the fractional samples at optimal direction θ have to be even sampled $x^e[i,j]$. Generally, the interpolation is described as,

$$x^e[i + sign(n-1)tan\theta, j+n] = \sum_k a_k . x^e[i+k, j+n] \tag{7}$$

where k's are the number of integer pixels around $sign(n-1)\theta$ and a_k's are the interpolation filtering coefficients. For prediction and update steps samples from six nearest even rows are utilized [20]. If optimal direction crosses over the integer sample the value is estimated by the nearest even sample otherwise the fractional sample is calculated from interpolation of the two nearest even samples. The specific is given by (8),

$$x^e[i + sign(n-1)tan\theta, j+n] = \begin{cases} x^e[i + sign(n-1)tan\theta, j+n]; & \theta = 0, \pm 45 \\ 0.5.(x^e[i,j+n] + x^e[i + sign(n-1), j+n]); & \theta = \pm 22.5 \\ 0.5.(x^e[i,j+n] + x^e[i - sign(n-1), j+n]); & \theta = \pm 67.5 \end{cases} \tag{8}$$

To capture different face variations efficiently, an improved quadtree partitioning scheme is proposed to partition each face image into blocks of apparent directional details. All the samples in a quadtree partitioned block will have similar direction. The scheme provides an effective direction assignment and henceforth increases the efficacy of the prediction and update steps. Let each face image $x[i,j]$ is quadtree partitioned into non-overlapping blocks x_l with the initial block size S_{ini}. The minimum block size value as S_{min} and value of Lagrangian multiplier as γ are also considered. The energy summation of the prediction error from each block is calculated as,

$$PE_{l,n} = \sum_{i,j \in R_{l,n}} ||x_l[i,j] - R_{l,n}[i,j]||_2^2 + \gamma D^n \tag{9}$$

where $R_{l,n}[i,j]$ are the filtered directional responses obtained by applying the prediction filter W^p along the predefined directions θ. D^n is the number of bits spent on signaling the selection of directions. When a sample is predicted from the neighboring samples, each candidate direction is checked and the direction with the smallest prediction error is finally selected. The optimal direction which gives the minimum prediction error is obtained as,

$$\theta_l = argmin_n\{PE_{l,n}\} \tag{10}$$

The complexity of this partitioning is controlled by the value of Lagrangian multiplier γ i.e. if it is to zero a full partition quadtree is obtained and set to ∞ does not allow any partitioning [18]. But if one follow this method and continue partitioning then a full quadtree will be achieved every time. This method deteriorates the quadtree partitioning and direction assessment to each block. To

overcome this problem the improved quadtree partitioning scheme is proposed to facilitate face recognition problem as described in Algorithm 1. The above-mentioned 1-D process can be simply extended to the 2-D process where second dimension lifting is again performed on high-pass $H[i,j]$ and low-pass signals $L[i,j]$ to generate four sub-bands i.e. $LH(i,j)$, $LL(i,j)$, $HH(i,j)$, and $HL(i,j)$.

Algorithm 1: Improved quadtree partitioning scheme.

Input: Face image $x[i,j]$, initial block size S_{ini}, the minimum block size S_{min} for quadtree partitioning and the value of Lagrangian multiplier γ
Output: Quadtree partitioned face image and direction data.
Step 1: Quadtree partition the face image $x[i,j]$ into several blocks x_l of size S_{ini}
Step 2: for each block x_l **do**
2.1. Find the filtered directional responses denoted as $R_{l,n}$ with prediction filter W^p along the predefined direction θ_l
2.2. Calculate the energy summation of the prediction error energy $PE_{l,n}$ using (9) from the filtered directional responses
2.3. Calculate the optimal direction along which the minimum prediction error is obtained using (10)
2.4. Quadtree partitioned each sub-block x_l into four sub-blocks $x_{l,i}, i = 1,\ldots,4$
2.5. Repeat step 2.1 to 2.3 and find the prediction error energy $PE(x_{l,i})$
Step 3: if $PE(x_{l,i}) \geqslant PE(x_l)$ **&** $sizeof(x_{l,i}) = S_{min}$ **do**
3.1. Stop partitioning
3.2. Store the optimal direction θ_l and corresponding optimal block $x_{l,i}$
else Repeat step 2

$$HH[i,j] = g_{HH}.(H^o[i,j] - P_{2h}(H^e)[i,j]) \tag{11}$$

$$HL[i,j] = g_{HL}.(H^e[i,j] + g_{HH}^{-1}(U_{2h}(HH)[i,j])) \tag{12}$$

$$LH[i,j] = g_{LH}.(L^o[i,j] - P_{2l}(L^e)[i,j]) \tag{13}$$

$$LL[i,j] = g_{LL}.(L^e[i,j] + g_{LH}^{-1}(U_{2l}(LH)[i,j])) \tag{14}$$

$L^e[i,j]$ and $L^o[i,j]$ are the even and odd columns of 1-D low-pass signal $L[i,j]$. Similarly $H^e[i,j]$ and $H^o[i,j]$ are the even and odd columns of high-pass signal $H[i,j]$. P_{2h} and U_{2h} are the prediction and update operators applied to the high pass signal $H[i,j]$ in the second dimension lifting. P_{2l} and U_{2l} are the prediction and update operators applied to the low pass signal $L[i,j]$ in the second dimension lifting. g_{LL}, g_{LH}, g_{HL}, and g_{HH} are the scaling factors for normalizing the energy of four synthesis filters where $g_{LL} = g_L$ and $g_{HH} = g_H$. In the proposed work the same directions for first and second-dimensional lifting are utilized [17]. 2-D Conventional lifting wavelet transform can be viewed as a particular case of 2-D SADIWT when direction $\theta = 0$ [17]. Two face images of ORL database [32] and their quadtree partitioning scheme with direction estimation is presented in Fig. 1. 2-D SADIWT is described with term SADIWT from now onwards.

2.2. Completed local binary patterns (CLBP)

The local binary pattern (LBP) [6] initially proposed for extracting texture details, at present considered the most admired local descriptor for facial feature extraction [7,12–15,20,29,30]. To allocate a label for each pixel, the LBP operator uses its intensity value as a threshold and compares it against pixel values in a 3×3 neighborhood. Generally, the LBP is computed with P sampling points $(x_p \in (0 \ldots P-1))$ in the neighborhood of the center pixel x_m at a radial distance by R, as given in (15) [6],

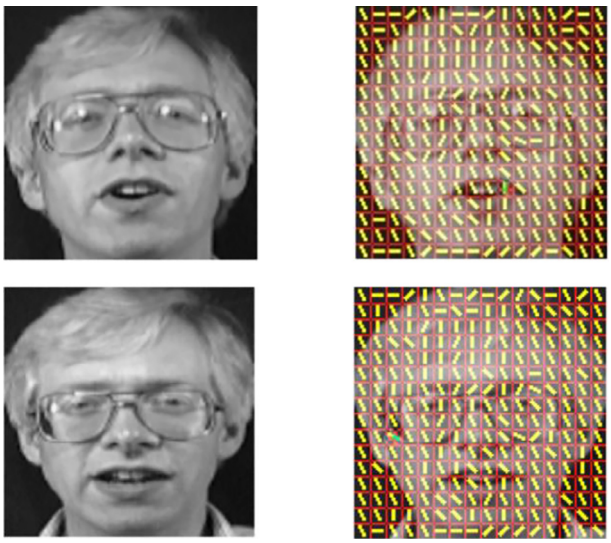

Fig. 1. Quadtree partitioning scheme and the direction estimation (ORL database).

$$LBP_{P,R} = \sum_{p=0}^{P-1} s.(x_p - x_m).2^p,\ s(diff) = \begin{cases} 1, & (diff) \geqslant 0 \\ 0, & (diff) < 0 \end{cases} \tag{15}$$

where $s(diff)$ is a threshold function. Fig. 2 depicts the LBP operator and the resultant label for the center pixel x_m. If the sampling points p's are not mapped in the neighborhood of the center pixel, they are bi-linearly interpolated [6]. Moreover, Ojala et al. [4] introduced a uniform patterns $LBP_{P,R}^{u2}$ where a binary pattern is uniform if it contains at most two bitwise transitions from 0 to 1, or vice versa when the binary pattern is considered circularly as given in (16),

$$U(LBP_{P,R}) = |s(x_{p-1} - x_m) - s(x_0 - x_m)| + \sum_{p=1}^{P-1} |s(x_p - x_m) - s(x_{p-1} - x_m)| \tag{16}$$

The $U(LBP_{P,R})$ value corresponding to the uniform pattern is smaller than two. In order to achieve rotation invariance based on $LBP_{P,R}^{u2}$, Guo et al. [8] defined the rotation invariant pattern $LBP_{P,R}^{riu2}$ as given in (17),

$$LBP_{P,R}^{riu2} = \begin{cases} \sum_{p=0}^{P-1} s.(x_p - x_m), & U(LBP_{P,R}) \leqslant 2 \\ P+1, & otherwise \end{cases} \tag{17}$$

where $U(LBP_{P,R})$ is calculated using (16). Thus there are $P+2$ different $LBP_{P,R}^{riu2}$ patterns. After $LBP_{P,R}^{riu2}$ labeling of the image pixels, codes of all pixels for an input image are collected and formed into a histogram [6]. A histogram of $LBP_{P,R}^{riu2}$ labeled image $x_{LBP}[i,j]$ can be defined as,

$$H_l = \sum_{i,j} F\{x_{LBP}[i,j] = l\},\ F\{A\} = \begin{cases} 1, & if\ A\ is\ true \\ 0, & if\ A\ is\ false \end{cases} \tag{18}$$

where $l = 0,1,2,\ldots,n-1$ and n is the number of different labels produced by the $LBP_{P,R}^{riu2}$ operator and the dimension of H_l is $P+2$. The LBP histogram H_l provides information about the local distribution of spots, edges over the entire image and can be used as an image feature descriptor [7].

To represent the local descriptive features further completely, Guo et al. [8] proposed CLBP where a local region is represented

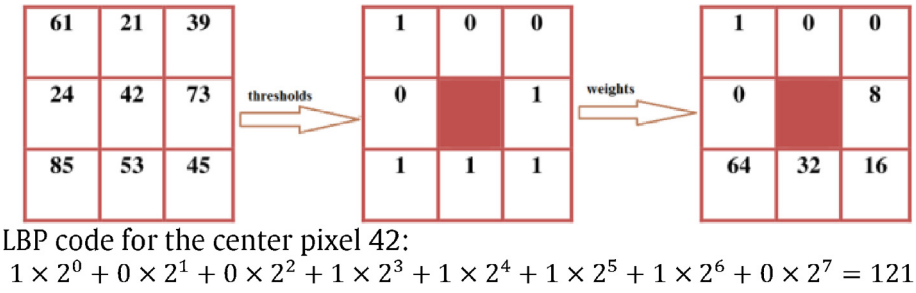

Fig. 2. LBP computation.

by its center pixel and a local difference sign magnitude transform (LDSMT). For a given pixel x_m in the image with x_p as its neighbors, a local difference can be calculated between x_p and x_m given as $D_p = x_p - x_m$. This local difference characterizes the image local structure at x_m. D_p can be further divided into parts as given in (19) [8],

$$D_p = S_p \times M_p \quad where, \; M_p = |D_p|, \quad \text{and} \quad S_p = \begin{cases} 1, & D_p \geqslant 0 \\ -1, & D_p < 0 \end{cases} \tag{19}$$

where S_p is the sign component of D_p, and M_p is the magnitude component of D_p. Let $CLBP\_S$ denote the LBP pattern for S_p [8]. $CLBP\_S$ operator is same as the original LBP operator which indicates the sign (positive or negative) of difference between the center pixel x_m and local neighboring pixels x_p.

$$CLBP\_S = \sum_{p=0}^{P-1} s.(x_p - x_m).2^p, \; s(diff) = \begin{cases} 1, & (diff) \geqslant 0 \\ 0, & (diff) < 0 \end{cases} \tag{20}$$

Subsequently, Guo et al. [8] defined the CLBP pattern for M_p, $CLBP\_M$ which is calculated same as $CLBP\_S$ but it deals with a difference of the magnitude.

$$CLBP\_M = \sum_{p=0}^{P-1} t(M_p, C).2^p, \; t(z, C) = \begin{cases} 1, & z \geqslant C \\ 0, & z < C \end{cases} \tag{21}$$

where C is the mean value of the M_p from the whole image. $CLBP\_M$ calculates the local variance of magnitude. The center pixel x_m which also expresses the image local gray level and consist of discriminative information, can be coded as $CLBP\_C$.

$$CLBP\_C = t(x_m - m_i) \tag{22}$$

where m_i is the mean value of the image. When $P = 8$, $R = 1$, and considering the rotation invariant uniform patterns, the illustration of $CLBP^{riu2}_{P,R}$ pattern is shown in Fig. 3. The dimension of $LBP^{riu2}_{P,R}$ defined in (17) is $P + 2$.

Thus the dimension of the histogram corresponding to $CLBP\_M^{riu2}_{P,R}$ is also $P + 2$. The dimension of the histogram corresponding to $CLBP\_S^{riu2}_{P,R}$ is also $P + 2$. The dimension of the histogram corresponding to $CLBP\_C^{riu2}_{P,R}$ is 2. As per the theory stated in [8], $CLBP\_S$, $CLBP\_M$, and $CLBP\_C$ histogram features can be combined jointly or hybridly. As compared to [30], in our proposed method the concatenation of $CLBP\_S$ and $CLBP\_M$ histogram features is performed and denoted as $CLBP\_S\_M^{riu2}_{P,R}$. The dimension of the histogram corresponding to $CLBP\_S\_M^{riu2}_{P,R}$ is $(P + 2) \times (P + 2)$. Certainly, $CLBP\_C$ also consist of some discriminative information [8] but, including it to form the feature set will increase the feature vector dimension and here it is to emphasize the fact that together with sign component $CLBP\_S$, magnitude component $CLBP\_M$ in CLBP facilitate to form an efficient local feature descriptor. For $P = 8$, $R = 1$, the illustration of the CLBP maps are shown in Fig. 4 for two CMU-PIE face database images [35,36].

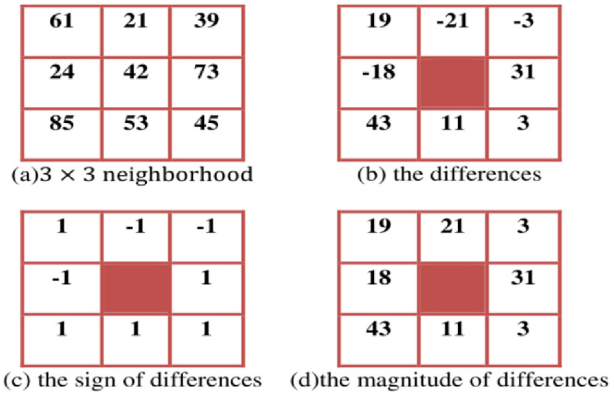

Fig. 3. Division of difference of CLBP.

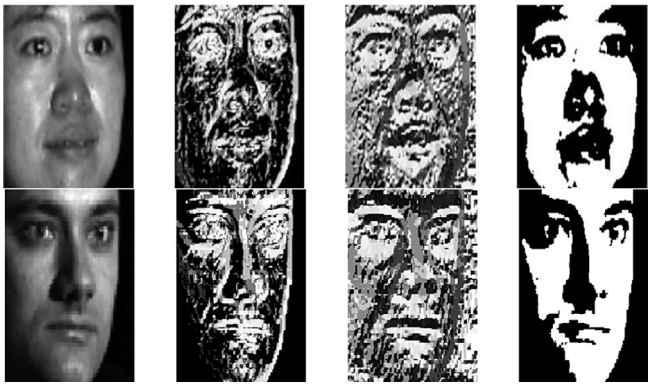

Fig. 4. CLBP patterns (From left to right: Original image, CLBP_M, CLBP_S, CLBP_C).

2.3. Classification based on collaborative representation

Wright et al. [24] developed SRC technique and achieved exceptional performance for face recognition. Given a test sample, SRC represents it as a sparse linear combination of training samples. To analyze SRC, Zhang et al. [25] developed CRC as a substitute approach. It is verified that it is the collaborative representation (CR), but not the $l1$-norm sparsity that makes CRC dominant for face classification [25]. CRC utilize all the training face images to linearly represent a test face image under the $l2$-norm minimization solution [25]. CRC has significantly less complexity than SRC [25]. Here the CRC method is explained and its significance is discussed in our proposed method. Assume, there are N training samples from C classes with each class having n_k training samples and $X_k = [x_{k,1}, x_{k,2}, \ldots, x_{k,n_k}] \in \mathbb{R}^{m \times n_k}$ is the training sample matrix of kth class and m is the dimension of the sample. In CRC any test sample $y \in \mathbb{R}^{m \times 1}$ from kth class with a dictionary $X \in \mathbb{R}^{m \times n_k}$ can be collaboratively represented as a linear combination of all the training samples as given in (23),

$$y = \alpha_{1,1}x_{1,1} + \alpha_{1,2}x_{1,2} + , \ldots , + \alpha_{c,c}x_{c,c} \tag{23}$$

The collaborative representation coefficient vector $\hat{\alpha}$ is obtained by solving the following regularization minimization objective function [25] as given in (24),

$$\hat{\alpha} = argmin_{\alpha}\{\|y - X\alpha\|_2^2 + \lambda\|\alpha\|_2^2\} \tag{24}$$

where λ is the regularization parameter. As verified by [25], CRC uses $l2$-norm instead of $l1$-norm in the regularization solution and $\alpha \in \mathbb{R}^{m\times 1}$ is considered as a collaborative representation of y in terms of X. The solution of CR with regularized least square in (24) can be easily derived as given in (25) [25].

$$\hat{\alpha} = (X^T X + \lambda I)^{-1} X^T y \tag{25}$$

Let $P = (X^T X + \lambda I)^{-1} X^T$. Due to the independency of P with y, it can be pre-calculated as a project matrix [24]. Thus, whenever test sample arrives it is simply projected on to P via Py, which makes CRC faster compared to SRC. Considering the $l2$-norm of $\hat{\alpha}$, CRC uses the following classification criterion to assign the test sample y to the kth object class based on a minimum regularized reconstruction error [25] as given in (26)

$$identity(y) = argmin_k \left\{ \frac{\|y - X_k\hat{\alpha}_k\|_2}{\|\hat{\alpha}_k\|_2} \right\} \tag{26}$$

If the testing feature vector is formed from a non-variant face image, the estimated coding vector $\hat{\alpha}$ is sparse even if $l2$-norm is used for regularization term. However, the testing feature vector extracted from face images contains various variations due to expression, pose, and illumination. These variations may harm the sparseness of the coding vector $\hat{\alpha}$. At this point, error function can accurately estimate the error of the testing feature vector and henceforth the identity. This fact strengthens our selection of CRC as a classification method over SRC.

3. Proposed face recognition method

The face images are affected by numerous variations such as expression, pose, and illumination which make the task of any face recognition method intricate. So it is significant to devise a method to deal with these variations efficiently. In the proposed method, SADIWT is proposed which efficiently provides the multi-resolution features from quadtree partitioned sub-blocks based on the image characteristics. Moreover, CLBP is applied to the SADIWT selected sub-bands which additionally provides the local descriptive features from the sub-blocks of the sub-bands. Next, CRC method is performed on these local descriptive features to perform a robust classification which improves the overall performance. In this section, the proposed method is illustrated which utilizes SADIWT with proposed seven directions along with the improved quadtree partitioning scheme and CLBP as a local feature descriptor followed by the application of CRC for effective classification.

Accordingly, SADIWT entails two separable transforms, i.e. separable vertical and horizontal lifting-based transform in the optimal direction. 2-level decomposition of SADIWT is performed to obtain the top-level's low-frequency sub-band coefficient matrix *LL* and high-frequency sub-band coefficient matrices (*LH*, *HL*, *HH*). The *LL* sub-band due to SADIWT implementation retains most of the information of the face image. But the sub-bands *LH* and *HL* also contain edge details along horizontal and vertical directions. Thus to efficiently capture the local descriptive features using the CLBP, *LH* and *HL* sub-bands are also considered with *LL* sub-band.

HH sub-band is neglected here as it mostly contains the noise with negligible feature information. Fig. 5 depicts the general structure of the proposed method. As discussed in the earlier section, the proposed improved quadtree partitioning scheme partitions each face image into non-overlapping blocks and proposed filtering directions as mentioned in (6) are correlated in each block based upon the facial description. The prediction and update lifting operations as given in (1) and (3) are executed in the direction of edges in these non-overlapping blocks. Whilst performing the prediction and update step, if a fractional sample arrives, a sub-pixel interpolation scheme as described in (8) is performed to calculate this fractional sample value. The sub-pixel interpolation is used to improve the directional orientation property of the image. Due to the adaptive direction selection from quadtree partitioned blocks, dependencies observed over image discontinuities can be successfully de-correlated which tend to concentrate the energy of high-frequency sub-bands into low-frequency *LL* sub-band [17]. Moreover, for the edges existing at diagonal directions, the SADIWT algorithm performed along these edges also decreases the energy in high-frequency sub-bands *LH* and *HL*. However, *LH* and *HL* sub-band also provide information relative to the edge and contour which can support to extract pose, expression, and illumination-relevant feature details. With the inclusion of *LH* and *HL* sub-bands along with *LL* sub-band to extract CLBP-based histogram features, most of the details of the face variations can be acquired to form a significant feature vector which helps to deal with various face variations.

When applied for the whole face image CLBP histogram features only provide the micro-pattern without describing their location information. Sustaining the details about the local spatial relationship is very important for pose and expression feature extraction. Moreover due to pose and expression variations intra-class differences may be larger than inter-class differences which in turn decrease the classification accuracy.

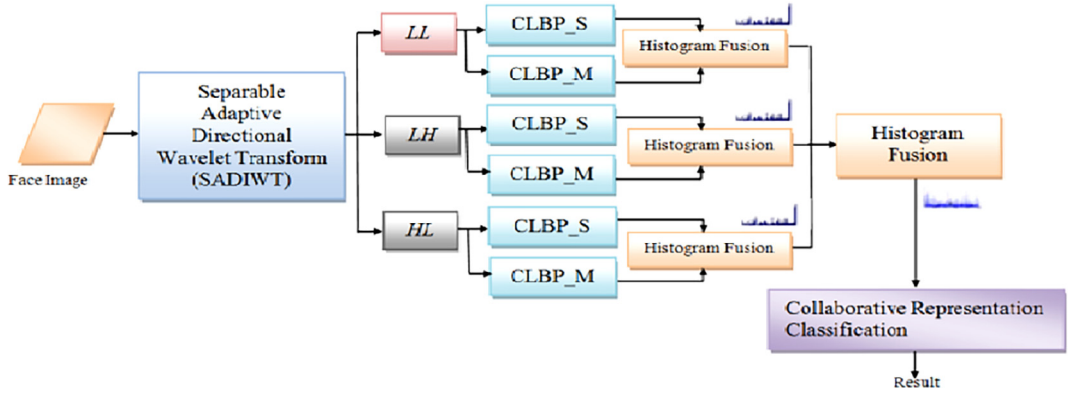

Fig. 5. General structure of the proposed method.

To overcome this problem one instinctive solution is to use multi-region information, as information from different regions provides complementary information for classification. For this, each sub-band is equally divided into small regions. Thus, the top level's SADIWT sub-bands i.e. *LL*, *LH*, and *HL* sub-bands are divided into k non-overlapping rectangle regions $R_0, R_1, \ldots, R_{m-1}$, each of size $x \times y$ pixels. From each of these m regions, as noted in (20) and (21) rotation invariant uniform $CLBP\_S_{8,1}^{riu2}$ and $CLBP\_M_{8,1}^{riu2}$ histogram features are extracted and concatenated to construct the resultant histogram feature $CLBP\_S\_M_{8,1}^{riu2}$. The $CLBP\_S\_M_{8,1}^{riu2}$ from all these regions are concatenated into a single spatially enhanced histogram feature vector. Let $LL\_H_{l,k}$, $LH\_H_{l,k}$, and $HL\_H_{l,k}$ denote such concatenated spatially enhanced histogram feature vectors for *LL*, *LH*, and *HL* sub-bands respectively,

$$LL\_H_{l,k} = \sum_{i,j} F\{LL_{CLBP}[i,j] = l\} F\{[i,j] \in R_k\} \tag{27}$$

$$LH\_H_{l,k} = \sum_{i,j} F\{LH_{CLBP}[i,j] = l\} F\{[i,j] \in R_k\} \tag{28}$$

$$HL\_H_{l,k} = \sum_{i,j} F\{HL_{CLBP}[i,j] = l\} F\{(i,j) \in R_k\} \tag{29}$$

where, $l = 0, 1, 2, \ldots, n-1$, $k = 0, \ldots, m-1$. LL_{CLBP}, LH_{CLBP}, and HL_{CLBP} denote the CLBP coded image of *LL*, *LH*, and *HL* sub-bands respectively. The dimension of histogram feature vector $CLBP\_S\_M_{8,1}^{riu2}$ for each region is $(P+2) \times (P+2)$. The histograms feature vector $CLBP\_S\_M_{8,1}^{riu2}$ from successive regions are concatenated to form a feature set for a particular sub-band and its feature dimension is calculated as $(P+2) \times (P+2) \times k$. Similarly, all the histogram features from all the three sub-bands are concatenated to form the spatially enhanced histogram feature vector $CLBP\_S\_M_{fv}$.

$$CLBP\_S\_M_{fv} = [LL\_H_{l,k}, LH\_H_{l,k}, HL\_H_{l,k}] \tag{30}$$

As each face image is resized to 128×128 pixels uniform size for face images of all the face databases. Each of the generated SADIWT sub-bands (*LL*, *LH*, *HL*) is of size 32×32 pixels. In our proposed method each of these sub-bands is divided into $k = 16$ regions with $x \times y = 8 \times 8$ pixels region and thus the combined dimension of $CLBP\_S\_M_{fv}$ is $10 \times 10 \times 16 \times 3 = 4800$. To notify once again only the sign component *CLBP_S* and the magnitude component *CLBP_M* of the CLBP operator are considered to obtain the histogram features. This representation not only captures the local texture edge details but also considers the magnitude variance of the three sub-band coefficients. As a result, multi-resolution analysis based dense local variations in terms of CLBP-based histogram features are efficiently extracted.

Algorithm 2 explains the different steps of the proposed method. To reduce the dimension of the histogram feature vectors, PCA is applied while performing the CRC. Considering the class label of training image as input, the objective of face classification method is to discriminate the class of a test face image. Thus, referring to the previous theory of CRC, there are C classes with each class having n_k training samples. Every training sample x_{k,n_k} is obtained from the learning stage of the CLBP histogram feature extraction step which is a one dimensional feature vector $CLBP\_S\_M_{fv}$. Thus the feature vector dictionary obtained from C classes is described as $X_k = [x_{k,1}, x_{k,2}, \ldots, x_{k,n_k}] \in \mathbb{R}^{m \times n_k}$, where m is the dimension of each feature vector $CLBP\_S\_M_{fv}$. Let $y \in \mathbb{R}^{m \times 1}$ is the testing feature vector from the kth class obtained from the testing stage of the CLBP histogram feature extraction step. According to CRC once the dictionary X is learned from the training dataset X_k, the collaborative representation coefficient vector $\hat{\alpha}$ of the test feature y can be computed by solving the regularization minimization objective function as mentioned in (24). The solution of $\hat{\alpha}$ can be easily calculated using (25). Considering the $l2$-norm of $\hat{\alpha}$, CRC uses the classification criterion mentioned in (26) to assign the test sample y to the kth class. Thus finally, the test feature is classified as the existing class via collaborative representation coding.

Algorithm 2: Proposed face recognition method.

Input: Train image, test Image, SADIWT decomposition level J, CLBP block size, the value of λ for CRC
Output: Classification accuracy
Step 1: Preprocessing
1.1. Read input face image X
1.2. Perform RGB to gray level conversion if the face image is not grayscale
1.3. Resize the image to 128×128 pixel resolution
Step 2: Computation of SADIWT sub-bands
for a number of decomposition level J **do**
2.1. Perform steps 1 to steps 3 of Algorithm 1 to obtain the quadtree partitioned image and direction data
2.2. Perform the SADIWT decomposition with the prediction and the update operations in the selected directions in the selected block
2.3. Obtain SADIWT sub-bands (*LL*, *LH*, *HL*) and proceed with *LL* sub-band for the next decomposition level
end for
Step 3: Completed Local Binary Patterns(CLBP) Computation
3.1 Consider the top-level's (*LL*, *LH*, *HL*) sub-bands and split each sub-band into non-overlapping regions R_k each with size 8×8
for each sub-band **do**
for each sub-block within the sub-band **do**
for each coefficient value within the sub-block **do**
3.2. Compute the $CLBP\_M_{8,1}^{riu2}$ and $CLBP\_S_{8,1}^{riu2}$ histogram features from each region R_k using (20) and (21) respectively
3.3. Concatenate the $CLBP\_S_{8,1}^{riu2}$ and $CLBP\_M_{8,1}^{riu2}$ histogram features form each region to form one histogram feature vector $CLBP\_S\_M_{8,1}^{riu2} = [CLBP\_S_{8,1}^{riu2}, CLBP\_M_{8,1}^{riu2}]$
3.4. Concatenate all such $CLBP\_S\_M_{8,1}^{riu2}$ multi-region histogram feature vectors to form the enhanced histogram feature vector for *LL*, *LH*, and *HL* sub-bands using (27)–(29) respectively
end for end for end for
3.5. Concatenate all the sub-band histogram feature vectors $LL\_H_{l,k}$, $LH\_H_{l,k}$, and $HL\_H_{l,k}$ to form the spatially enhanced histogram feature vector $CLBP\_S\_M_{fv}$ using (30)
Step 4: Collaborative representation Classification (CRC)
4.1. Save the feature vector $CLBP\_S\_M_{fv}$ to train feature vector database $CLBP\_S\_M_{train}$
4.2. Perform dimensionality reduction using PCA [2] for the $CLBP\_S\_M_{train}$ feature vector database
4.3. Save the $CLBP\_S\_M_{train}$ feature vector database to reduced feature database X_k in the CRC method
4.4. Repeat Step 1 to 3 on each test image to obtain the discriminant test feature vector y in the CRC method
4.5. Normalize the columns of X_k and y to have the unit $l2$-norm
4.6. Find the collaborative representation using (25) and output the identity of the test feature y using (26) and thus calculate the classification accuracy

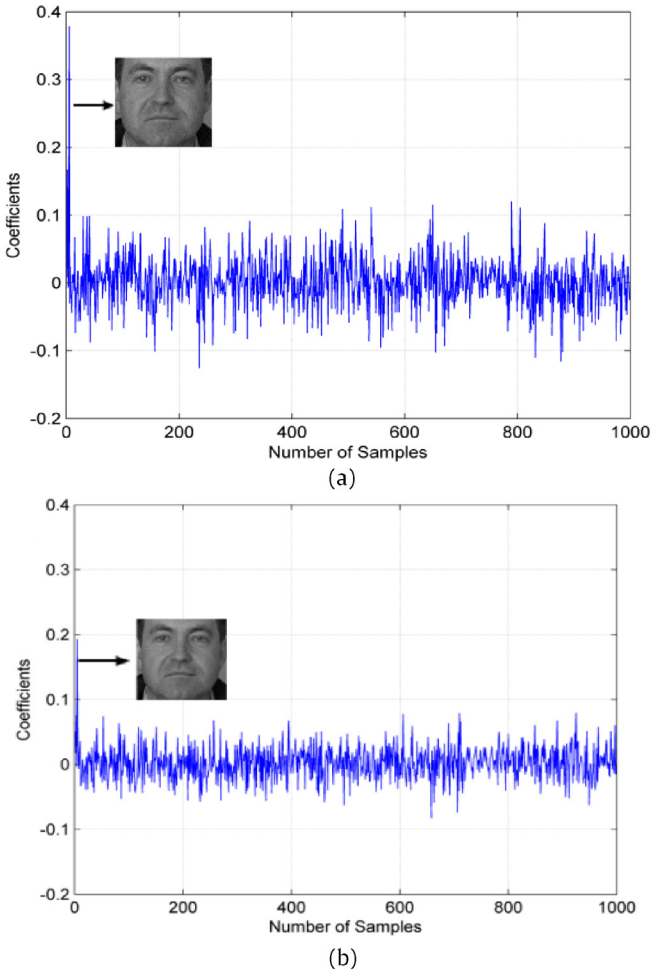

Fig. 6. (a) the representation coefficients obtained by CRC and (b) the final representation coefficients obtained by the proposed method.

Fig. 6 depicts the coding coefficients for a test face image belonging to the first class from the FERET face database [33,34]. These coefficients are obtained by CRC and the proposed method on 1000 training images of 200 subjects from FERET face database. Fig. 6(a) shows the CRC representation coefficient for this test image. Fig. 6 (b) shows the final representation coefficient for the test image using the proposed method. A legal test image has non-zero representation entries mostly concentrated on one subject, whereas an illicit test image has coefficients distributed widely among multiple subjects. Without any pre-processing step and considering only the raw samples, the CRC method produces large non-zero coefficients entries corresponding to training samples from many different classes for few numbers of training samples from each class. Whereas, in our proposed method the local discriminant feature vectors obtained from the former step when applied for CRC, improve its performance and thus the test image can be represented by a lesser number of elements of the dictionary as shown in Fig. 6(b). For most of the test samples, the same result can be achieved in many experiments on the face databases. Obviously, the class-wise reconstruction errors of our proposed method will also exhibit its superior representation ability for classification tasks.

4. Experimental results

In this section, the performance of the proposed method is validated with variations in expression, illumination, and pose and compared it with various contemporary methods. Face databases composed under controlled conditions such as ORL [32], FERET [33,34], and CMU-PIE face database [35,36] are used. Face database such as LFW database [37–39] is also considered to demonstrate the performance of the proposed method for face images captured in un-controlled scenarios. Since proposed method utilizes CLBP histogram feature extraction from SADIWT sub-bands with CR classification, it is compared with various methods which not only include holistic and LBP-based descriptors but also include various representation methods. These methods include NN [23], LDA [3], LPP [5], LBP [7], WLD [9], SRC [24], CRC [25], LLC [11], LRC [26], and SRC-GSLBP [29]. A comparison with few LBP-based non-adaptive MRA face recognition methods such as LGBPHS [12], CTLBP [13], SPT-LBP [14], and GTCLBPSRC [30] is also additionally reported here. All the experiments randomly select few face images to form the training set and select remaining face images to form the test set. Each experiment is repeated 10 times and the average classification accuracy is recorded. PCA is used as the dimensionality reduction method for CRC, SRC, LRC, and in our proposed method. For SRC implementation the *l*1_*ls* [40] package is used.

4.1. Parameter settings

All experiments are conducted using MATLAB R2014a on a standard i3-2120, 3.30 GHz machine with a 2.0 GB RAM and 64-bit operating system. Some parameter settings are required to efficiently implement SADIWT method. The decomposition level J to perform SADIWT is selected as two for all the databases. To efficiently capture the local directions from the quadtree partitions blocks, initial block size S_{ini}, minimum block size S_{min}, and the value of Lagrangian multiplier are also selected. With reference to [19,20], $S_{ini} = 8 \times 8$ pixel size is selected for all the databases. In addition, the value of the Lagrangian multiplier as 9 and the value of minimum block size $S_{min} = 4 \times 4$ pixel size is selected for all the databases [19,20]. Extensive experiments are conducted to verify the effectiveness of these values and established to be optimum for all the databases. The size of the region for extracting the CLBP local feature descriptor is considered as 8×8 pixels. For NN, LDA, and LPP based methods the NN classifier with Euclidean distance measure is used. For LBP and LGBPHS images are partitioned into the 8×8 pixel regions. For LGBPHS, filters at five different scales and eight orientations are applied [12]. For LBP method, uniform pattern $LBP^{u2}_{8,1}$ is used [7] and NN classifier with Chi-square distance measure is adopted. For WLD, a patch size of 3×3 pixel is considered for coding and generated histograms of differential excitation and orientation component are concatenated into a 2-D histogram [20]. For SRC-GSLBP, hierarchal multiscale LBP is used to form the feature set and SRC with matching pursuit-based greedy search strategy is implemented with reference to the original paper. The value of regularization parameter λ in SRC, CRC, LLC, and in our method is set to 0.01, 0.01, 0.001, and 0.01 respectively to obtain the best results [10]. For CTLBP similar methodology is adopted as mentioned in [13] to form the feature set and LPP is applied with NN classifier. For SPT-LBP similar feature extraction steps are applied. LLB is used to reduce the feature dimension along with Chi-square as the similarity measure [14]. For implementing GTCLBPSRC with reference to the original paper, Gabor filters with five orientations and four scales are used and all three CLBP components are used to form the histogram features. Regularization parameter for GTCLBPSRC is set to 0.01 [30].

4.2. Experiment on the ORL face database

The ORL database is composed of 400 face images from different subjects (10 different images per subject) with some variations in

Fig. 7. Sample face images of a subject from the ORL face database.

pose and facial expressions. Each image is resized to 128×128 pixel size. Fig. 7 suggests some sample images of a subject. A random subset with L ($L = 2, 3, 4, 5$) images per subject is selected to form a training set and the remaining images per subject are selected to form a testing subset. This procedure is repeated ten times and the average classification accuracies are listed in Table 1. The results demonstrate the effectiveness of the proposed method in capturing directional MRA-based local descriptive features for faces with variations in expression and pose. For a small database like the ORL database, it is apparent that high accuracy is achieved by all the methods as the number of subjects in the testing set is not very high. With the increase in the number of training samples the classification accuracy also increases for all methods but the proposed method yields superior result even for fewer numbers of training samples. To capture the spatial structure information related to expression and pose, SADIWT sub-bands are split into 8×8 pixel regions and CLBP-based histogram features are obtained from these regions. The multi-region enhanced histogram features add local discrimination and application of CRC on these features improves the classification accuracy.

Improvement of 20.35%, 17.91%, and 16.95% is reported over NN, LDA, and LPP respectively if two samples per subject are randomly used to form the training set. Improvement of 9.18% and 7.65% is observed over LBP and WLD respectively when the number of training samples per subject is randomly selected as five.

Table 1
Classification accuracies of different methods on the ORL face database (%).

Number of training samples per subject	2	3	4	5
NN	70.59	74.30	80.42	84.21
LDA	72.75	75.07	82.33	85.33
LPP	73.60	78.53	88.47	91.70
LBP	68.44	78.21	87.08	89.00
WLD	73.13	81.43	87.50	90.50
SRC	81.31	83.14	85.83	87.50
CRC	81.25	83.21	88.33	88.50
LLC	83.72	86.71	90.33	91.40
LRC	75.89	80.23	84.47	86.50
SRC-GSLBP	85.31	90.20	95.23	97.00
LGBPHS	83.06	85.86	93.75	95.00
CTLBP	82.81	87.86	94.50	95.50
SPT-LBP	86.04	89.22	93.66	97.18
GTCLBPSRC	86.25	89.57	94.58	97.50
Proposed method	88.62	91.28	95.83	98.00

Improvement of 10.71%, 9.69%, 6.73%, and 11.73% over SRC, CRC, LLC, and LRC is observed when the number of training samples per subject is randomly selected as five. LGBPHS, CTLBP, and SPT-LBP methods do not offer adaptive direction estimation relating to face variations whereas SADIWT method performs direction adaptation effectively with face variations. When the number of training samples per subject is randomly selected as two, improvement of 6.27%, 6.55%, and 2.91% is observed over LGBPHS, CTLBP, and SPT-LBP respectively. LGBPHS is computationally expensive. CTLBP uses only the LBP coded image of the approximation sub-band and does not consider the multi-region information. SPT-LBP method exhibits comparable classification accuracy but the feature selection process is threshold dependent. The proposed method consists the benefit of performing rapid classification using CRC over SRC which is used as the classification method in SRC-GSLBP and GTCLBPSRC. An improvement of 3.7% and 2.67% is observed over SRC-GSLBP and GTCLBPSRC respectively when the number of training samples per subject is randomly selected as two. The proposed method has the benefit of rapid classification due to CRC as compared to SRC-GSLBP and GTCLBPSRC.

4.3. Experiment on the FERET face database

The FERET database consists of 14,126 facial images from 1199 subjects, which are dissimilar across ethnicity, gender, and age. This database is selected to consider a large number of face images with pose and expression variation. A subset of this database is adopted which includes 200 subjects with expression and pose variations [10,29,30]. Each subject has seven images that differ from each other in pose (left and right tilting with 15° and 25°), one frontal image with expression variation and one frontal image with illumination variation. Face images of a subject are as shown in Fig. 8. Each image is resized to 128×128 pixel size. A random subset with L ($L = 3, 4, 5$) images per subject is selected to form a training set and the remaining images per subject are selected to form a testing subset. This procedure is repeated for ten times and the average classification accuracies are listed in Table 2. Similar to ORL database a comparison is also performed with various methods to establish the efficacy of the

proposed method. Extraction of multi-region CLBP histogram features from SADIWT sub-bands and application of CRC improves the classification accuracy substantially. The proposed method achieves highest classification accuracy even for fewer numbers

Fig. 8. Sample face images of a subject from the FERET face database.

Table 2
Classification accuracies of different methods on the FERET face database (%).

Number of training samples per subject	3	4	5
NN	22.54	31.13	44.33
LDA	27.00	34.75	49.50
LPP	39.41	58.00	63.51
LBP	34.67	57.00	59.50
WLD	44.82	57.28	61.41
SRC	32.18	44.86	54.64
CRC	35.16	47.75	56.50
LLC	36.52	49.60	58.30
LRC	31.91	42.24	53.00
SRC-GSLBP	56.32	69.00	75.25
LGBPHS	48.67	59.50	69.25
CTLBP	49.10	67.12	73.75
SPT-LBP	63.07	74.30	78.65
GTCLBPSRC	61.67	71.80	80.10
Proposed method	63.50	74.67	80.25

of training images as compared to other methods. When the number of training samples per subject is randomly selected as three, the proposed method suggests an impro-vement of 64.50%, 57.48%, and 37.93% over NN, LDA, and LPP respectively. LBP and WLD also demonstrate a reduced performance as compared to the proposed method. When the number of training samples per subject is randomly selected as five an improvement of 31.91%, 29.59%, 27.35%, and 33.95% in classification accuracies of SRC, CRC, LLC, and LRC can be observed respectively which confirm the effectiveness of the proposed method over these classification methods.

The LBP-based non-adaptive MRA methods such as LGBPHS, CTLBP, and SPT-LBP do not provide adaptation in selecting a direc-tion within a block of samples and also have a limitation in terms of high computational cost and complex filter design. Moreover, LBP-based local histogram features, when extracted from LGBPHS, CTLBP and SPT-LBP sub-bands, do not suffice in representing the features as compared to our proposed method. The improvement of our method over LGBPHS, CTLBP, and SRC-GSLBP is 13.71%, 8.10%, and 6.23% respectively if the number of training samples per subjects is randomly selected as five. A comparison with recently proposed GTCLBPSRC also confirms the efficacy of the proposed method. Here we report an improvement for less number of samples but as the number of samples increases, GTCLBPSRC provides a close classification accuracy to proposed method but at the expense of more computational time. Thus with this set of the experiment, we can demonstrate that the proposed method also works well for a database with a large number of face images under pose and expression variations.

4.4. Experiment on the CMU-PIE face database

This database is considered to assess the adequacy of our proposed method under the state of illumination with pose variations. This is a large database which contains 41,368 face images of 68 subjects. The face images exhibit 13 dissimilar poses and 43 dissimilar illumination variations with 4 dissimilar expressions [35,36]. For our experimentation, the database considered here is a subset of CMU-PIE database of one near frontal pose C05 wherein all the images are under different illuminations and expressions [28]. The subset C05 incorporates 68 subjects and each subject has 49 face images. Each image is manually aligned and resized to 128×128 pixel size. Fig. 9 gives some samples face images of a subject from this database.

A random subset with L ($L = 5, 6, 7, 8$) images for each subject is selected to form the training set, and the remaining images for each subject are selected to form the testing set. Table 3 enumerates the classification accuracies for different methods. It is evident that the proposed method surpasses different methods. This is because the foremost challenge of this database is illumination and expression and the proposed method can make an adaptive selection of best lifting direction from the proposed direction set as given in (6) and uses interpolated samples to predict as per local characteristics of the face image. The proposed directions are adequate to reap all the essential illumination and expression relevant information from the face images. The interpolation is performed at the spatial resolution of seven directions which preserves the local details of illumination-variant features. The CLBP operator sufficiently extracts local structural details from the SADIWT sub-bands. Moreover, CRC on receiving such local descriptive features assures efficient classification. Hence establishes our method efficient in approximating the illumination and expression related features. NN, LDA, LPP fail to represent the illumination and expression related features as these methods treat the face image as a whole and provide reduced performance. LBP and WLD do provide multi-region information and show some improvement but still drop behind to the proposed method. For LBP and WLD improvement of 5.5% and 4.78% is observed when the number of training samples per subject is randomly selected as eight.

For SRC, CRC, LLC, and LRC an improvement of 5.71%, 4.72%, 5.67%, and 7.85% respectively, can be observed when the number of training samples is randomly selected as eight. Illumination

Table 3
Classification accuracies of different methods on the CMU-PIE face database (%).

Number of training samples per subject	5	6	7	8
NN	70.08	75.41	78.36	82.25
LDA	81.05	82.63	84.31	87.66
LPP	82.23	83.69	85.63	88.70
LBP	81.12	85.57	88.62	90.71
WLD	84.56	86.76	90.44	91.43
SRC	85.40	87.39	88.27	90.53
CRC	86.41	87.77	89.83	91.48
LLC	83.60	85.62	88.20	90.58
LRC	83.53	84.53	86.48	88.48
SRC-GSLBP	87.25	91.12	92.60	94.34
LGBPHS	86.47	89.23	92.14	93.37
CTLBP	85.30	90.70	91.25	93.69
SPT-LBP	88.00	92.04	93.35	95.20
GTCLBPSRC	88.66	92.30	94.10	95.37
Proposed method	88.97	92.61	94.57	96.02

Fig. 9. Sample face images of a subject from the CMU-PIE Pose05 face database.

and expression mainly affect the edge manifold of the image. LBP-based non-adaptive MRA methods such as LGBPHS, CTLBP, SPT-LBP, and GTCLBPSRC do not consider edge manifolds adaptively and extracted histogram features do not capture such details efficiently. We observe improvement over SRC-GSLBP and GTCLBPSRC which depicts the effectiveness of the generated histogram features using the proposed method for illumination and expression-variant face images.

4.5. Experiment on the LFW face database

The LFW [37–39] is a huge database which contains 13,233 face images of 5749 eminent personalities in unconstrained conditions with extreme variations of pose, orientation, illumination, expression, accessories, and background which makes it a challenging database for face recognition [37]. In the present work, an aligned version LFW-a of the LFW database is selected [38]. LFW-a aligns all the images using a commercial face alignment software [39]. A subset is created which collects no less than 10 dissimilar images of 158 subjects from the LFW-a database as mentioned in [10,31]. Some examples of this subset are presented in Fig. 10. Each image is resized to 128 × 128 pixel size.

A subset with L (L = 3, 4, 5, 6, 7) images per subject is randomly selected to form the training set, and rest images per subject are selected to form the testing set. Classification accuracies of different methods are listed in Table 4. Since the images are collected in the unconstrained environment the classification accuracies are low in this database. Due to large face variations, this database imposes an immense challenge, but the result of our proposed method is excep-tionally promising. The adaptation of directional selection as per the image characteristics allows the sub-bands of SADIWT to preserve most of the directional information from the face images and in turn capture the face variations in a great detail. Additionally, owing to the application of CLBP on SADIWT sub-bands, pose, illumination and facial expression details can be successfully extracted and an efficient feature descriptor is composed. Moreover, considering these efficient local descriptive features as input, CRC improves the overall classification accuracy of the proposed method. Our proposed method exhibits an improvement of 65.80%, 59.95%, 52.41%, 26.68%, and 23.20% in classification accuracies for NN, LDA, LPP, LBP, and WLD respectively when the number of training samples per subject is randomly selected as seven.

Similarly, when five samples for each subject are selected randomly, we observe improvement of 16.94%, 9.74%, 19.74%, and 24.89% over SRC, CRC, LLC, and LRC respectively. Specifically, the improvement in performance demonstrated by our method is significant for less number of training images. For instance, when training images per subject are three our method achieves a classification accuracy of 32.64% which is higher than the classification accuracy achieved by other methods. It is evident from Table 4 that our method outperforms LGBPHS, CTLBP, and SPT-LBP methods in extracting local directional multi-resolution features and demonstrates improvement of 27.69%, 21.38%, and 4.94% respectively when three samples per subject are selected randomly to form the training set. We observe comparable improvement over SRC-GSLBP and GTCLBPSRC which depicts the effectiveness of sparse representation methods. But due to CRC implementation, the computation time is less for our proposed method. This experiment demonstrates the effectiveness and robustness of the proposed method for face recognition in the unconstrained condition. Here one point needs to be emphasized that strict and standard features will create sparser coefficients with collaborative representation (CR) which improves the classification accuracy.

Table 4
Classification accuracies of different methods on the LFW-a face database (%).

Number of training samples per subject	3	4	5	6	7
NN	7.11	12.85	14.43	15.23	19.19
LDA	8.59	13.35	15.21	18.35	22.47
LPP	9.61	14.50	18.14	22.67	26.70
LBP	21.97	23.10	29.24	37.18	41.14
WLD	22.06	24.72	30.20	39.92	43.09
SRC	23.67	31.25	35.64	42.38	47.90
CRC	27.30	34.60	38.73	43.19	48.73
LLC	26.90	31.31	34.44	41.73	46.10
LRC	25.16	30.43	32.23	35.71	40.09
SRC-GSLBP	30.42	37.13	39.40	44.20	54.05
LGBPHS	23.60	32.67	34.93	38.84	42.33
CTLBP	25.66	34.28	38.49	41.14	46.62
SPT-LBP	31.03	37.80	40.10	45.51	54.60
GTCLBPSRC	31.55	38.27	40.42	45.63	55.00
Proposed method	32.64	39.66	42.91	46.52	56.11

4.6. Single image per person (SIPP)

Due to non-availability of training face images, practical face recognition system usually suffers from single image per person (SIPP) problem [25]. To solve the lack of samples problem, CRC utilizes the training faces from all the classes to represent the test face. The collaborative representation algorithm helps to reduce the representation error. This fact strengthens the decision to select CRC as the classification method in our proposed method. Here, to validate this and to handle the SIPP we conducted this experiment.

One image per subject is selected randomly as the training image and rest images per subject are selected as the test images. It is shown in Table 5 that performance of the proposed method is better than different comparative methods for all the databases. LDA, LPP, and CTLBP cannot deal with SIPP problem, thus their results are not reported here. For FERET database, improvement of 19.08%, 8.05%, and 5.51% is observed for SRC-GSLBP, SPT-LBP, and GTCLBPSRC respectively. Whereas, for LFW-a database, improvement of 15.08%, 14.03%, and 9.06% is observed for SRC-GSLBP, SPT-LBP, and GTCLBPSRC respectively. Thus for SIPP problem, the improvement of our method is noticeable for all the databases. This is due to the fact that SADIWT extracts directional multi-resolution features and the CLBP when performed on SADIWT sub-bands, extract local descriptive features. Additionally,

Fig. 10. Sample face images of a subject from the LFW-a face database.

Table 5
Classification accuracies for SIPP for different face databases (%).

Method	ORL	FERET	CMU-PIE	LFW-a
NN	58.80	18.24	7.71	4.41
LBP	57.24	29.20	10.47	6.52
WLD	62.13	32.50	12.00	7.12
SRC	65.28	31.74	19.52	8.20
CRC	66.67	31.91	20.40	9.35
LLC	67.82	32.40	17.22	8.80
LRC	63.58	28.43	15.65	6.22
SRC-GSLBP	72.20	45.23	25.00	13.68
LGBPHS	67.95	37.18	24.40	9.07
SPT-LBP	73.77	51.40	26.05	13.85
GTCLBPSRC	74.00	52.82	26.45	14.65
Proposed method	75.83	55.90	27.02	16.11

CRC considers the correlation among these local descriptive features which eventually increase the classification accuracy.

4.7. Face recognition with occlusion

In order to further analyze the robustness of the proposed method with occlusions, an experiment is conducted on LFW-a face database. A randomly located square block with "Baboon" image is inserted into the test images as an adjoining block occlusion from 10% to 40% [24]. To perform this experiment seven randomly selected images per subject are used as training images and the rest three images are used as test images. Fig. 11 illustrates the face image from LFW-a face database with blocking occlusion ratio of 10%, 20%, and 30%.

Table 6 illustrates the classification accuracies of different comparative methods with blocking occlusion ratio from 10% to 40%. With the increase of image occlusion rate from 10% to 40%, one can observe a descending tendency in the classification accuracy. For a complex database like this and even in the presence of extreme occlusion our method delivers reasonable classification accuracy. Though SRC-GSLBP, SPT-LBP, and GTCLBPSRC can achieve comparable classification accuracy, even at 40% occlusion the proposed method still performs better. For our proposed method, the results indicate that the correlation information maintained by CRC compensates the occluded part information in the test images and helps to improve the classification accuracy of the proposed method.

Fig. 11. Examples of random partial block occlusion.

Table 6
Classification accuracies of different methods for random partial occlusions on LFW-a face database (%).

Method	10%	20%	30%	40%
NN	13.29	12.45	6.85	4.43
LDA	16.11	13.34	11.40	6.25
LPP	23.32	19.66	15.12	9.80
LBP	38.90	27.75	24.83	16.29
WLD	40.08	31.43	27.69	21.42
SRC	43.23	40.56	32.85	22.77
CRC	44.72	41.77	33.54	23.00
LLC	42.12	39.29	29.85	20.08
LRC	38.27	34.77	27.54	18.50
SRC-GSLBP	49.40	44.86	40.20	31.91
LGBPHS	40.59	35.40	29.33	22.00
CTLBP	44.84	41.14	37.76	29.11
SPT-LBP	48.32	45.80	39.87	32.25
GTCLBPSRC	49.00	46.64	40.08	32.66
Proposed method	51.68	47.46	44.52	33.12

4.8. Comparison with the different direction sets

In order to verify the validity of the proposed direction set in the implementation of SADIWT, a comparison is established with other adaptive directional transform methods such as DIW with five directions [18] and ADWT with nine directions [19] and Similar settings are considered from section 4.1 such as decomposition level, initial block size S_{ini}, and the value of the Lagrangian multiplier. Furthermore, for a fair comparison similar settings for CLBP and CRC are also applied for histogram feature extraction and classification respectively.

To perform this experiment, for all the databases five randomly selected images per subject are used as the training images and the rest images are used as the test images. Results illustrated in Table 7 demonstrate that the proposed direction set considers the face image characteristics more efficiently as compared to the direction set of [18,19]. The local edges and boundaries of the face image provide descriptive features which are efficiently captured with the proposed direction set with sub-pixel interpolation step. Improved quadtree partitioning scheme and SADIWT performed in the adaptively selected optimal direction within the optimal block increases the classification accuracy. The directions mentioned in [19] only consider the distant integer samples which result in directions that are too sparse to characterize the original image features. For ORL and FERET databases the improvement in classification accuracy is 2.55%, 2.43% respectively over ADWT. For CMU-PIE database the improvement over ADWT and DIW is 3.5% and 2.61% respectively. For the LFW-a database, the methods using the direction set [18,19] provides close accuracies to the proposed method but proposed method performs better.

This improvement indicates that more directions increase the computational complexity and fewer directions cannot extract essential characteristics from face images. The proposed method with proposed seven directions with interpolation-based SADIWT and improved quadtree partitioning scheme helps to improve the performance reasonably.

4.9. Computational complexity

Consecutively, to demonstrate that the proposed method is computationally efficient, the computation time for feature extraction step of various comparative methods is calculated. Table 8 shows the computation time of various comparative methods to process the ORL database face image of size 128×128 pixel resolution. Only feature extraction step is applied i.e. no further classification step is applied. Mainly those methods are considered which require the pre-processing at the feature extraction step. One can see the proposed method has a comparable computational

Table 7
Classification accuracies for different directions set (%).

Database	ADWT	DIW	Proposed method
ORL	95.50	97.00	98.00
FERET	78.30	79.14	80.25
CMU-PIE	85.82	86.65	88.97
LFW-a	41.50	41.22	42.91

Table 8
Comparison of different methods in terms of computation time for ORL database.

Method	Computation Time (s)
LBP	0.6
WLD	0.72
SRC-GSLBP	1.4
LGBPHS	1.8
CTLBP	1.1
SPT-LBP	1.18
GTCLBPSRC	2
Proposed method	1.2

time for feature extraction compared with different methods. The GTCLBPSRC method has the highest computation time.

5. Conclusion

In this paper, a face recognition method based on a proposed implementation of interpolation-based SADIWT is presented. In the implementation of SADIWT, we proposed to apply seven directions with an improved quadtree partitioning scheme to extract directional multi-resolution features from face images containing different face variations. Completed local binary patterns (CLBP) are applied on the selected top-level's SADIWT sub-bands to extract the multi-region local descriptive features in terms of spatially enhanced histogram features. In the proposed method we used CRC as the classification method which when performed on the local descriptive features obtained from the previous step demonstrate an efficient classification and improves the classification accuracy with great extent.

Experiments conducted on ORL, FERET, CMU-PIE, and LFW-a databases demonstrate the efficacy of our proposed method. The classification accuracy of the proposed method is compared with various methods which include holistic, prominent representation and some LBP-based non-adaptive MRA methods. The proposed method offered an improvement over NN, LDA, and LPP methods for all the databases. Representation methods, for instance, SRC, CRC, LLC, and LRC are also implemented and compared with the proposed method. A comparison with LBP-based non-adaptive MRA methods such as LGBPHS, CTLBP, SPT-LBP, and GTCLBPSRC also demonstrates the efficiency of the proposed method.

Based on the experiments performed on different databases particularly for complex face variations, such as CMU-PIE and LFW-a, the proposed method achieves significantly higher classification accuracy and outperforms other comparative even for a fewer number of training samples. This work also demonstrates the robustness and discrimination capability in handling SIPP and random block occlusion problem. In a nutshell, this work provides an effective face recognition method under the influence of expression, illumination, and pose variation and presents SADIWT as an alternate efficient adaptive MRA method for feature extraction.

Acknowledgments

The authors are very grateful to the editors and anonymous reviewers for insightful comments and valuable suggestions to improve the quality, which has been incorporated in this manuscript.

References

[1] A.K. Jain, S. Prabhakar, An introduction to biometric recognition, IEEE Trans. Circuits Syst. Video Technol. 14 (1) (2004) 4–20.
[2] M. Turk, A. Pentland, Eigenfaces for recognition, J. Cognit. Neurosci. 3 (1) (1991) 71–86.
[3] P.N. Belhumeur, J.P. Hespanha, D.J. Kriegman, Eigenfaces vs. Fisherfaces: recognition using class specific linear projection, IEEE Trans. Pattern Anal. Mach. Intell. 19 (7) (1997) 711–720.
[4] Z.H. Huang, W.J. Li, J. Wang, T. Zhang, Face recognition based on pixel-level and feature-level fusion of the top-level's wavelet sub-bands, Info. Fusion 22 (2015) 95–104.
[5] X. He, S. Yan, Y. Hu, P. Niyogi, H.J. Zhang, Face recognition using laplacian faces, IEEE Trans. Pattern Anal. Mach. Intell. 27 (3) (2005) 328–340.
[6] T. Ojala, M. Pietikäinen, T. Maenpää, Multi-resolution gray-scale and rotation invariant texture classification with local binary patterns, IEEE Trans. Pattern Anal. Mach. Intell. 24 (7) (2002) 971–987.
[7] T. Ahonen, A. Hadid, M. Pietikäinen, Face description with local binary patterns: application to face recognition, IEEE Trans. Pattern Anal. Mach. Intell. 28 (12) (2006) 2037–2041.
[8] Z.H. Guo, L. Zhang, D. Zhang, A completed modeling of local binary pattern operator for texture classification, IEEE Trans. Image Process. 19 (6) (2010) 1657–1663.
[9] J. Chen, S. Shan, C. He, et al., WLD: a robust local image descriptor, IEEE Trans. Pattern Anal. Mach. Intell. 32 (9) (2010) 1705–1720.
[10] Z. Zhang, L. Wang, Q. Zhu, S.K. Chen, Y. Chen, Pose-invariant face recognition using facial landmarks and weber local descriptor, Knowl.-Based Syst. 84 (2015) 78–88.
[11] J. Wang, J. Yang, K. Yu, et al., Locality-constrained linear coding for image classification, in: Proceedings of IEEE International Conference on Computer Vision and Pattern Recognition, 2010, pp. 3360–3367.
[12] W. Zhang, S. Shan, W. Gao, H. Zhang, Local Gabor binary pattern histogram sequence (LGBPHS): a novel non-statistical model for face representation and recognition, in: Proceedings of IEEE International Conference and Computer Vision, 2005, pp. 786–791.
[13] L. Zhou, W. Liu, Z.M. Lu, T. Nie, Face recognition based on curvelets and local binary pattern features via using local property preservation, J. Syst. Softw. 95 (2014) 209–216, https://doi.org/10.1016/j.jss.2014.04.037.
[14] A. Alelaiwi, W. Abdul, M.S. Dewan, M. Migdadi, G. Muhammad, Steerable pyramid transform and local binary pattern based robust face recognition for E-health secured login, Comput. Electr. Eng. 53 (2016) 435–443, https://doi.org/10.1016/j.compeleceng.2016.01.008.
[15] H.Y. Patil, A.G. Kothari, K.M. Bhurchandi, Expression invariant face recognition using local binary patterns and contourlet transform, Optik 127 (2016) 2670–2678.
[16] C.L. Chang, B. Girod, Direction-adaptive discrete wavelet transform for image compression, IEEE Trans. Image Process. 16 (5) (May 2007) 1289–1302.
[17] W. Ding, F. Wu, X. Wu, S. Li, H. Li, Adaptive directional lifting-based wavelet transform for image coding, IEEE Trans. Image Process. 16 (2) (Feb. 2007) 416–427.
[18] A. Maleki, B. Rajaei, H.R. Pourreza, Rate-distortion analysis of directional wavelets, image processing, IEEE Trans. Image Process. 21 (2) (Feb. 2012) 588–600.
[19] In Press Accepted Manuscript Muqeet, M.A., Holambe, R.S. Local appearance-based face recognition using adaptive directional wavelet transform. Journal of King Saud University – Computer and Information Sciences, 2017, http://dx.doi.org/10.1016/j.jksuci.2016.12.008.
[20] In Press Accepted Manuscript, Muqeet, Mohd. Abdul, Holambe, R.S., Local binary patterns based on directional wavelet transform for expression and pose-invariant face recognition, Appl. Comput. Inform. (2017), https://doi.org/10.1016/j.aci.2017.11.002.
[21] W. Sweldens, The lifting scheme: construction of second generation wavelets, SIAM J. Math. Anal. 29 (2) (1998) 511–546.
[22] J. Kovacevic, W. Sweldens, Wavelet families of increasing order in arbitrary dimensions, IEEE Trans. Image Process. 9 (3) (2000) 480–496.
[23] R. Duda, P. Hart, D.Stork, Pattern Classification, second ed., 2001.
[24] J. Wright, A. Yang, et al., Robust face recognition via sparse representation, IEEE Trans. Pattern Anal. Mach. Intell. 31 (2) (2009) 210–227.
[25] L. Zhang, M. Yang, X.C. Feng, Sparse representation or collaborative representation: Which helps face recognition?, in: Proceedings of IEEE International Conference on Computer Vision, 2011, pp 471–478.
[26] I. Naseem, R. Togneri, M. Bennamoun, Linear regression for face recognition, IEEE Trans. Pattern Anal. Mach. Intell. 32 (11) (2010) 2106–2112.
[27] F. Cao, H. Hu, J. Lu, J. Zhao, Z. Zhou, J. Wu, Pose and illumination variable face recognition via sparse representation and illumination dictionary, Knowl.-Based Syst. 107 (2016) 117–427.
[28] Z. Fan, M. Ni, Q. Zhu, E. Liu, Weighted sparse representation for face recognition, Neurocomputing 151 (1) (2015) 304–309.
[29] Z. Liu, X. Song, Z. Tang, A novel SRC fusion method using hierarchical multi-scale LBP and greedy search strategy, Neurocomputing 151 (2015) 1455–1467.
[30] X. Wang, Q. Zhu, J. Cui, Y. Wang, Sparse representation method based on Gabor and CLBP, Optik 124 (2013) 5843–5850.
[31] P. Zhu, L. Zhang, Q. Hu, S.C. Shiu, Multi-scale patch based collaborative representation for face recognition with margin distribution optimization, in: Computer Vision–ECCV 2012, Springer, 2012, pp. 822–835.
[32] http://www.cl.cam.ac.uk/research/dtg/attarchive/facedatabase.html.
[33] P.J. Phillips, H. Wechsler, J. Huang, P. Rauss, The FERET database and evaluation procedure for face recognition algorithms, Image Vis. Comput. 16 (1998) 295–306.
[34] P.J. Phillips, H. Moon, S.A. Rizvi, P.J. Rauss, The FERET evaluation methodology for face recognition algorithms, IEEE Trans. Pattern Anal. Mach. Intell. 22 (2000) 1090–1104.

[35] W.H. Yang, D.Q. Dai, Two-dimensional maximum margin feature extraction for face recognition, IEEE Trans. Syst., Man, Cybern., Part B: Cybern. 39 (4) (2009) 1002–1012.
[36] J.R. Beveridge, B.A. Draper, J.M. Chang, M. Kirby, et al., Principal angles separate subject illumination spaces in YDB and CMU-PIE, IEEE Trans. Pattern Anal. Mach. Intell. 31 (2) (2009) 351–356.
[37] G.B. Huang, M. Ramesh, T. Berg., E. Learned-Miller, Labeled face in the wild: a database for studying face recognition in unconstrained environments Technical Report, 07-49, Univ. of Massachusetts, Amherst, 2007.
[38] http://www.openu.ac.il/home/hassner/data/LFW-a/.
[39] L. Wolf, T. Hassner, Y. Taigman, Similarity scores based on background samples, Computer Vision–ACCV 2009 (2010) 88–97.
[40] S. Kim, K. Koh, M. Lustig, S. Boyd, D. Gorinevsky, An interior-point method for large-scale l1-regularized least squares, IEEE J. Select. Top. Signal Process. 1 (2007) 606–617.
[41] R. Eslami, H. Radha, Design of regular wavelets using a three-step lifting scheme, IEEE Trans. Signal Process. 58 (4) (April 2010) 2088–2101.